



DOI:10.22144/ctujoisd.2023.051

## Preparation and characterization of magnetic-lignin nanoparticles with potential applications for drug delivery

Cao Luu Ngoc Hanh<sup>1\*</sup>, Luong Huynh Vu Thanh<sup>1</sup>, Dang Huynh Giao<sup>1</sup>, Ho Quoc Phong<sup>1</sup>,  
Vo Thi Nhu Y<sup>2</sup>, and Dang Thi Viet Anh<sup>2</sup>

<sup>1</sup>College of Engineering, Can Tho University, Viet Nam

<sup>2</sup>Graduate student, College of Engineering, Can Tho University, Viet Nam

\*Corresponding author (clnhanh@ctu.edu.vn)

### Article info.

Received 19 Apr 2023

Revised 25 Apr 2023

Accepted 28 Apr 2023

### Keywords

$Fe_3O_4$ , magnetic-lignin nanoparticles, nanolignin

### ABSTRACT

*This study successfully combined  $Fe_3O_4$  nanoparticles (made by co-precipitation technique) and lignin (extracted from sugarcane bagasse) as magnetic-lignin nanoparticles. The factors affecting the synthesis such as ratio of  $Fe_3O_4$ /lignin and reaction time were investigated.  $Fe_3O_4$ @lignin nanoparticles were obtained at optimal conditions, including the ratio between  $Fe_3O_4$  and lignin of 1:0.5 and the reaction time of 9 hours. The resulting nanoparticles were spherical and had a fairly uniform particle size distribution, with an average diameter of  $53.42 \pm 5.12$  nm (obtained from SEM images). The thermal stability of  $Fe_3O_4$ /lignin nanoparticles is quite stable and lignin content in hybrid  $Fe_3O_4$ /lignin particles is estimated to account for about 32.82%. FTIR results show a successful combination of  $Fe_3O_4$  and lignin. The magnetic saturation of  $Fe_3O_4$ /lignin nanoparticles was determined by a vibrating sample magnetometer (VSM) with values of  $50.8 \text{ emu.g}^{-1}$ , showed that the material keeps its super-paramagnetic properties, which is critical for their application in drug delivery field.*

## 1. INTRODUCTION

In the previous study (Hanh, 2022) lignin nanoparticles from bagasse were successfully synthesized and showed initial success in the loading and release of curcumin at different pH environments. Lignin nanoparticles have potential applications in drug delivery. However, these lignin nanoparticles are still limited in targeted drug delivery. This is also the reason it is necessary to combine with one of the other targeting factors, such as magnetic particles (Figueiredo, 2017), folate targeting factor (Liu, 2018), thermo-sensitive factor (Kim, 2010), pH-sensitive factor (Zhao, 2020).

Among the above targeting factors,  $Fe_3O_4$  nanoparticles have super-paramagnetic properties, high maximum magnetic saturation value with a nano-scale and high homogeneity (Hasany, 2013).

$Fe_3O_4$  nanoparticles are often synthesized by co-precipitation to produce nanoparticles because of the simple and easy processing. However, at the nano-scale, the magnetic nanoparticles have a very large surface area and very high surface tension, resulting in the nanoparticles are often unstable and stick together, making it difficult to disperse in the water environment or converted to  $\gamma\text{-}Fe_2O_3$  in the presence of atmospheric environment. To overcome,  $Fe_3O_4$  nanoparticles also need to be coated with nanolignin on the outside to prevent decomposition, oxidation or dehydration of the magnetic nanoparticles to widen potential applications in numerous fields, especially in targeted drug delivery.

There are various studies on  $Fe_3O_4$  magnetic nanoparticles wrapped by an outer shell of materials such as chitosan, silica ( $SiO_2$ ), calcium

hydroxyapatite (HA), graphene oxide (GO). In 2019, Thang et al. studied the structural, morphological and properties of  $\text{Fe}_3\text{O}_4$  magnetic nanoparticles synthesized by thermal decomposition method. Next, the beads are coated with poly acrylic acid. The obtained materials have uniform size, average size of 10 nm, from saturation of 64.01 emu/g, good dispersion in the aqueous phase and have prospects for biomedical applications. In 2017, Ha et al. synthesized  $\text{Fe}_3\text{O}_4/\text{SiO}_2$  adsorbent materials by pyrolysis of  $\text{Fe}(\text{NO}_3)_3$  salts in  $\text{C}_2\text{H}_5\text{OH}$ ,  $\text{CH}_3\text{COOH}$  and medium capillary carrier  $\text{SiO}_2$  with good adsorption capacity of Cr(VI) in wastewater at a low pH. In 2020, Hoa et al. fabricated composite materials based on nano-chitosan/ $\text{Fe}_3\text{O}_4$  applied to lead treatment in aqueous solution. The obtained material is ~200 nm with 20-30 nm  $\text{Fe}_3\text{O}_4$  nanoparticles attached to chitosan particles.

Figueiredo et al. (2017) combined iron or iron oxide with lignin to deliver poorly water-soluble drugs. The pH of the release medium affects the kinetics of drug release for hydrophobic drugs, and drug release at pH 5.5 and 7.4 is over 90% uniform in the first 6 h. In the same year, Lin et al. synthesized lignin nanoparticles as an environmentally friendly carrier for drug release of resveratrol.  $\text{Fe}_3\text{O}_4$  nanoparticles are combined with the poorly water-soluble medication resveratrol for use in targeted cancer therapy. For four days, there was an 80% continuous drug release from the granules. Both the magnetic beads and the particles' anti-cancer activity had no negative effects on mice or cells. In 2019,  $\text{Fe}_3\text{O}_4$  nanoparticles were loaded on lignin nanoparticles prepared by Min et al. by self-assembly. Under optimal conditions,  $\text{Fe}_3\text{O}_4@\text{LNPs}$  showed a sensitive colorimetric detection of  $\text{H}_2\text{O}_2$  between 5 – 100  $\mu\text{M}$  and a 2  $\mu\text{M}$  detection limit. Its high catalytic activity allows it to be used promisingly in a variety of applications. However, the obtained particles have a relatively large average size (~152.8 nm). In 2020, Pei et al. synthesized  $\text{Fe}_3\text{O}_4@\text{lignin}$  nanoparticles by Mannich method, these particles are used as a substitute for phenol to prepare electromagnetic wave absorbing adhesive, which can be applied in plywood production. In 2021, without the use of organic solvents or functionalization lignin, Vasquez et al. synthesized  $\text{lignin}@\text{Fe}_3\text{O}_4$  by assembling kraft lignin into magnetic nanoparticles based on pH-oriented precipitation. These particles have a heterogeneous, multi-core magnetic structure, with the core formed by the aggregation of numerous  $\text{Fe}_3\text{O}_4$  magnetic nanoparticles and the shell of kraft lignin. The study

was carried out with the main objective of synthesizing magnetic lignin nanoparticles by combining  $\text{Fe}_3\text{O}_4$  nanoparticles and nanolignin extracted from sugarcane bagasse. The synthesized nanoparticles are determined in terms of size, shape, structure and properties to show potential applications in the field of targeted drug delivery.

## 2. MATERIALS AND METHOD

### 2.1. Materials

Xilong supplied ferrous chloride tetrahydrate ( $\text{FeCl}_2 \cdot 4\text{H}_2\text{O}$ , 99%), ferric chloride hexahydrate ( $\text{FeCl}_3 \cdot 6\text{H}_2\text{O}$ , 99%), sodium hydroxide (NaOH, 98%), sulfuric acid ( $\text{H}_2\text{SO}_4$ , 98%). Ethanol ( $\text{C}_2\text{H}_5\text{OH}$ , 99.5%) was bought from the Vietchem company. All chemicals were reagent grade and used as received. Sugarcane bagasse was obtained from a local sugar factory (Can Tho, Viet Nam).

### 2.2. Preparation of magnetic-lignin nanoparticles

#### 2.2.1. Preparation of $\text{Fe}_3\text{O}_4$ nanoparticles

Co-precipitation was used to synthesize  $\text{Fe}_3\text{O}_4$  nanoparticles. Thanh et al.' study (2021) served as the foundation for the synthesis process. Briefly, the amount of 1.217 g  $\text{FeCl}_3 \cdot 6\text{H}_2\text{O}$  and 0.448 g  $\text{FeCl}_2 \cdot 4\text{H}_2\text{O}$  were dispersed in 50 mL deionized (DI) water for 30 min with stirring 500 rpm and  $\text{N}_2$  purging at 80 °C. It was followed by the addition of 20 mL NaOH 2M. Finally, the sample was stirred for 90 min, washed with ethanol/water mixture (50/50 v/v) by sonication until neutral pH, dried for 2 h at 60°C, and stored at room temperature for further experiments.

#### 2.2.2. Preparation of lignin from sugarcane bagasse

Sugarcane bagasse was dried for 1 day and chopped about 0.5 - 1 cm. After that, bagasse is soaked with distilled water and heated in a thermostatic bath at 70°C for 2 hours to remove sugar. Bagasse was then dried for 24 hours at 60°C, ground finely and used to extract lignin (Arni, 2018). 20 g of bagasse after crushing is heated with 200 mL of 10% NaOH at 90°C for 90 minutes, then the residue is filtered to obtain black liquid. Slowly add 98%  $\text{H}_2\text{SO}_4$  into the black solution to form a light yellow precipitate, adjust the pH 2. Then, the sample was centrifuged at 5000 rpm for 15 minutes to obtain a precipitate. The precipitate was further washed with distilled water to pH 7. The sample was dried at 50°C for 24 h to obtain crude lignin. Dissolve 0.2 g of lignin in 10 mL of 70% ethanol solvent in a flask with a reflux

condenser system. After that, the mixture was heated to 50°C, kept for 20 minutes until the mixture was completely dissolved; a solution containing nanolignin chains was obtained.

### 2.2.3. Preparation of magnetic-lignin particles

The Fe<sub>3</sub>O<sub>4</sub> nanoparticles were added to water and ethanol with the ratio of 1:50:10 (w/v/v). Then, the mixture was ultrasonically vibrated for 15 minutes until the nanoparticles were evenly dispersed. The mixture was stirred at 600 rpm at 60°C and lignin was added slowly. The obtained Fe<sub>3</sub>O<sub>4</sub>/lignin nanoparticles were filtered, washed with deionized water and dried at 50°C for 24 h. The structure, morphology, thermal properties, and magnetic properties were determined via modern analytical methods.

### 2.2.4. Characterization

The particles deposited on the aluminum film were characterized directly using a scanning electron microscope (SEM, Hitachi S-4800). Using ImageJ software, the average size and particle size distribution were calculated based on the SEM results. After scraping off the aluminum film, the particles were distributed throughout the ethanol. To prevent particle agglomeration, the solution sample containing Fe<sub>3</sub>O<sub>4</sub>/lignin particles was ultrasonically treated for five minutes at 40°C. High-resolution transmission electron microscopy was used to assess the structure of the Fe<sub>3</sub>O<sub>4</sub>/lignin particles (HR-TEM, JEM 2100, JEOL, Japan). Under nitrogen flow, 32 scans and a resolution of 4 cm<sup>-1</sup> were used to record Fourier transform infrared (FTIR, Nicolet 100 Thermo Scientific) spectra on the device. Using a TGA/DSC3+, Mettler Toledo, with a heating rate of 10°C/min and an airflow rate of 20 mL·min<sup>-1</sup> at 100–800°C, the characteristic weight loss data were recorded. The magnetic properties of Fe<sub>3</sub>O<sub>4</sub> and Fe<sub>3</sub>O<sub>4</sub>/lignin were measured using a vibrating sample magnetometer (VSM, MicroSense EZ9 instrument, USA).

## 3. RESULTS AND DISCUSSION

### 3.1. Morphological properties of nano particles

The morphology and particle size distribution of Fe<sub>3</sub>O<sub>4</sub>@lignin nanoparticles at different reaction times and mass ratios were carried out by SEM and TEM. The reaction time and the weight ratio of Fe<sub>3</sub>O<sub>4</sub> to lignin were investigated because of their great influences on the magnetic-lignin nanoparticle formation. The reaction times investigated at 5 h, 7 h, and 9 h. The weight ratios of Fe<sub>3</sub>O<sub>4</sub> to lignin investigated at 1:0.5, 1:1, and 1:2 (Figure 1). In

general, all Fe<sub>3</sub>O<sub>4</sub>/lignin samples obtained are spherical and tend to agglomerate due to strong magnetic dipole interactions and characteristic Vander Waals forces of ferromagnetic particles. However, different reaction times and ratios between Fe<sub>3</sub>O<sub>4</sub> and lignin lead to materials with different diameters and particle size distributions.

At the reaction time of 5 h, the Fe<sub>3</sub>O<sub>4</sub> nanoparticles were almost not surrounded by lignin for all the investigated ratios between Fe<sub>3</sub>O<sub>4</sub> and lignin. The evidence is that most of the nanoparticles are close to the size of the Fe<sub>3</sub>O<sub>4</sub> nanoparticles (Ba-Abbad, 2022), while only a few larger particles are observed on the SEM images (Figure 1a-c). In addition, in the particle size distribution plot, the particle diameter is distributed from 10 to 60 nm and is usually concentrated in two value ranges (less than 15 nm and greater than 30 nm). When the reaction time was increased to 7 h, the particle diameter of most samples doubled compared to the samples with the reaction time of 5 h (e.g., in the sample Fe<sub>3</sub>O<sub>4</sub>:lignin = 1:2,  $d = 30.19 \pm 13.92$  nm at 5h, while  $d = 61.95 \pm 6.01$  nm at 7h). This implies that 7h is enough for the Fe<sub>3</sub>O<sub>4</sub> nanoparticles to be completely enveloped by lignin. The reaction time was further increased to 9h, the diameter of the samples tended to increase but not significantly (Figure 1g-i). The corresponding particle size distribution becomes more uniform. It showed that most of the Fe<sub>3</sub>O<sub>4</sub> nanoparticles were surrounded completely by lignin. Therefore, from the above results, it can be concluded that the optimal condition for the formation of Fe<sub>3</sub>O<sub>4</sub>/lignin particles is the ratio between Fe<sub>3</sub>O<sub>4</sub> and lignin of 1:0.5 and the reaction time of 9 hours. Under the above conditions, the resulting nanoparticles are spherical in shape, with an average size of  $53.42 \pm 5.12$  nm and a fairly uniform distribution of particle diameters. These results are also consistent with the study of Huang et al. (2020).

TEM images (Figure 2) show that the Fe<sub>3</sub>O<sub>4</sub> nanoparticles are successfully encapsulated by lignin, and after drying, formed consolidated clusters. Larger scaled images were also taken to show the homogeneity of the sample. The average size of the synthesized magnetic nanolignin under optimal conditions is  $34.25 \pm 15.04$  nm, according to TEM analysis. The diameter of Fe<sub>3</sub>O<sub>4</sub> nanoparticles observed with TEM is relatively smaller than that obtained from SEM ( $d = 53.42 \pm 5.12$  nm). This is explained because the TEM sample is dried, while the SEM sample is prepared on aluminium foil and dried naturally in air.

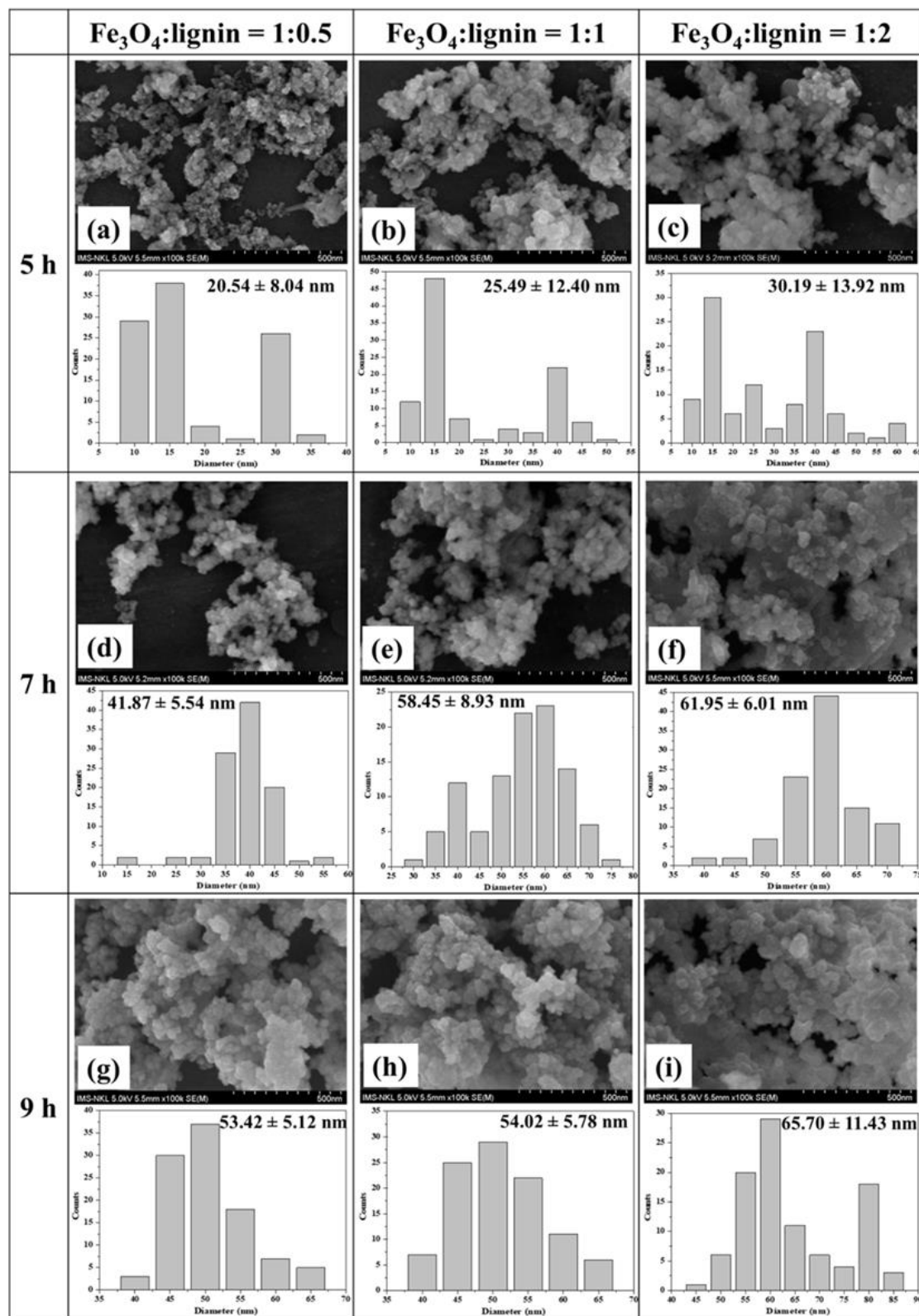
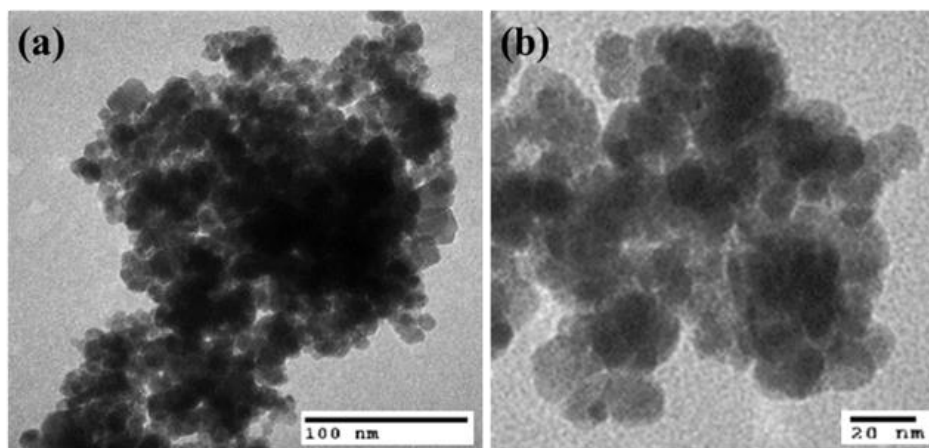


Figure 1. SEM images of  $\text{Fe}_3\text{O}_4/\text{lignin}$  nanoparticles at different reaction times and the weight ratio of  $\text{Fe}_3\text{O}_4$  to lignin; and the corresponding particle size distribution



**Figure 2.** TEM images of  $\text{Fe}_3\text{O}_4$ /lignin samples under optimal conditions with scale bar of (a) 100 nm and (b) 20 nm

### 3.2. FTIR analyses

By using FTIR analysis, the functional groups of lignin,  $\text{Fe}_3\text{O}_4$ , and  $\text{Fe}_3\text{O}_4$ /lignin were examined. Figure 3 displays the corresponding FTIR spectra. In contrast to lignin and  $\text{Fe}_3\text{O}_4$ , the band seen at  $573\text{ cm}^{-1}$  for  $\text{Fe}_3\text{O}_4$ /lignin is absent from the lignin spectrum and corresponds to the bending vibration of the Fe–O bond in the lattice of  $\text{Fe}_3\text{O}_4$ . This confirms that  $\text{Fe}_3\text{O}_4$  has been successfully combined with lignin. The peaks at  $702$  and  $938\text{ cm}^{-1}$  are attributed to the bending and amine vibration absorption peaks of the N–H bond. The peaks at

$1125$  and  $1327\text{ cm}^{-1}$  are characteristic for the syringyl ring and the C–O bond of the guaiacyl ring. A peak that was attributed to the lignin structure's methoxyl groups emerged at  $1417\text{ cm}^{-1}$ . The aromatic ring's vibrational bonds were detected at  $1491$  and  $1585\text{ cm}^{-1}$ . The stretching vibration and the -OH strain are connected to the absorption band at  $1667\text{ cm}^{-1}$ . In addition, a broad spectral range centered at  $3452\text{ cm}^{-1}$  characterizes the -OH group present in the aromatic ring, while the peak at  $2830\text{ cm}^{-1}$  characterizes the asymmetric C-H bond in the methylene group. This result corresponds to the results of Huang et al. (2020).

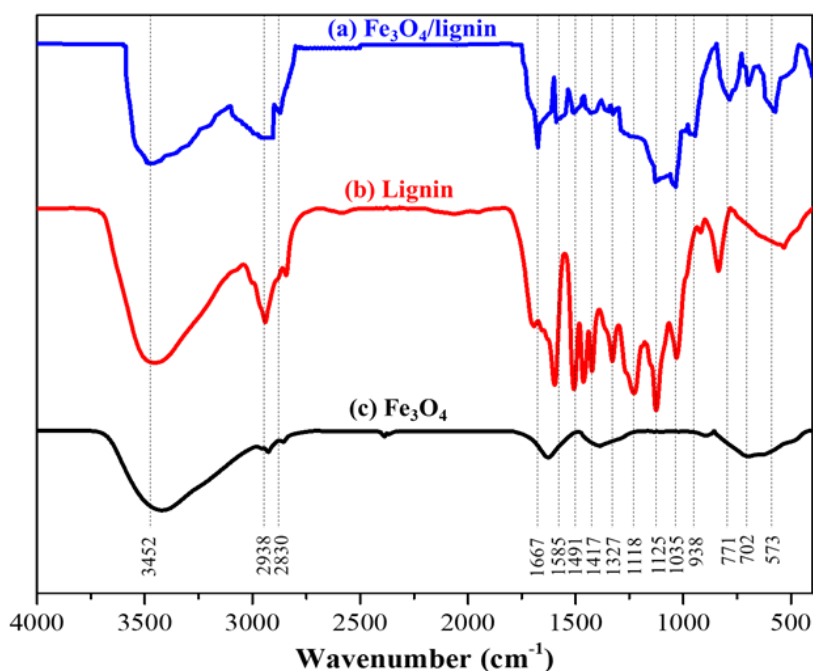


**Figure 3.** FT-IR spectra of (a)  $\text{Fe}_3\text{O}_4$ /lignin, (b) lignin, and (c)  $\text{Fe}_3\text{O}_4$

### 3.3. TGA analysis

The TGA curve analysis shown in Figure 4a demonstrates the extremely high thermal stability of  $\text{Fe}_3\text{O}_4$ . Based on the removal of physically bound water during the thermal treatment, the results show that this sample loses only about 7.24% of its mass. Three stages of degradation are visible in the lignin thermogram (Figure 4c). The first degradation step, which occurs between 0 and 220 °C and has a mass loss of about 10%, is associated with the local removal of water bonded to the lignin surface. In the temperature range of 220–650°C, the second mass loss of 68% is most likely related to the thermal breakdown of lignin macromolecules, which

involves the formation of new bonds due to crosslinking reactions or potentially the splitting off of oligomers. Above 650°C, there was a final and additional loss in sample weight due to lignin degradation and fragmentation. This sample's overall mass loss was calculated to be 87.38%. The total mass loss of the hybrid  $\text{Fe}_3\text{O}_4$ /lignin nanoparticles is 29.57% [= 32.82% – 3.25% (the mass loss of physical water)] at 200–800°C on the TGA curve (Figure 4b) and it can be predicted that this is the amount of lignin. Therefore, the remaining mass that is not decomposed by heat can be  $\text{Fe}_3\text{O}_4$ . This confirms the ability to combine  $\text{Fe}_3\text{O}_4$  and lignin successfully.

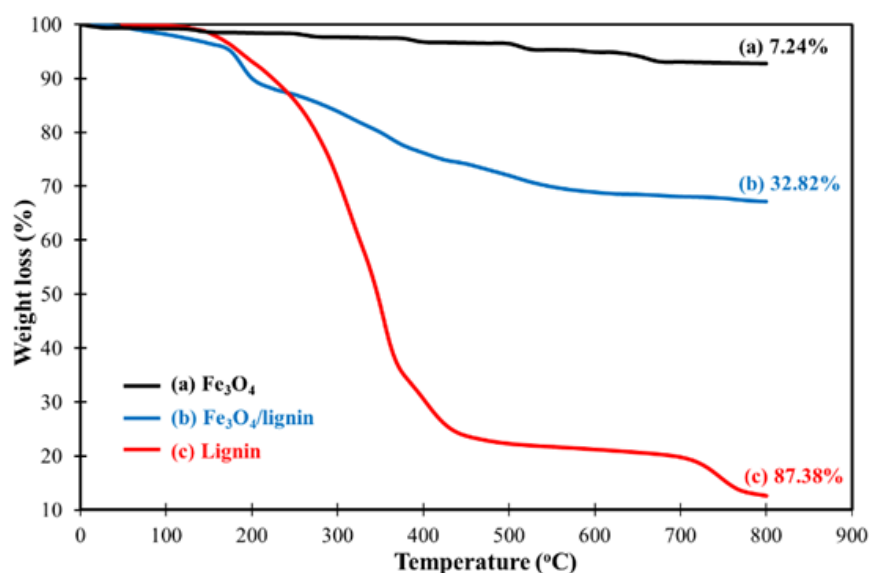
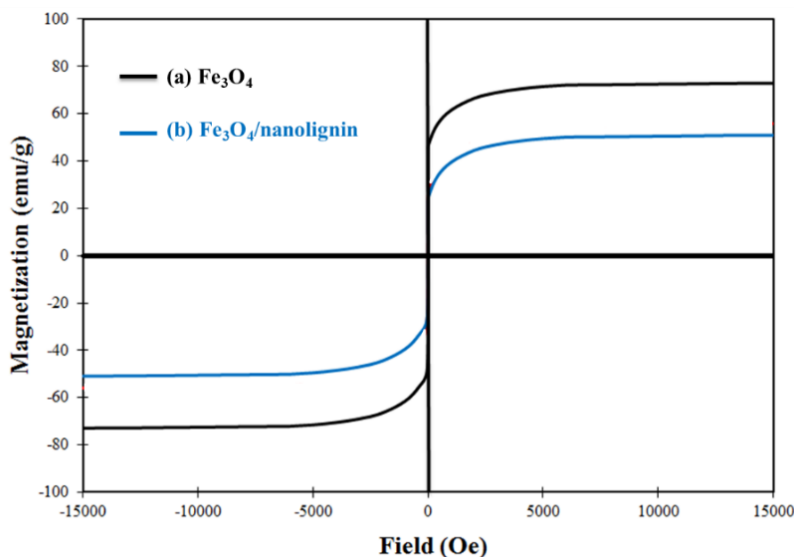


Figure 4. TGA profiles of (a)  $\text{Fe}_3\text{O}_4$ , (b)  $\text{Fe}_3\text{O}_4$ /lignin, and (c) lignin

### 3.4. Magnetic characterization

Lignin loading on the outer layer of  $\text{Fe}_3\text{O}_4$  nanoparticles has a significant impact on the magnetic strength of the particles in addition to directly affecting the iron distribution of the particles. Furthermore, the material recovery process will be directly impacted by the magnetic adsorbent's strength. As a result, Figure 5 depicts the magnetic strength of  $\text{Fe}_3\text{O}_4$  and  $\text{Fe}_3\text{O}_4$ /lignin after evaluation. The hysteresis loops of the  $\text{Fe}_3\text{O}_4$ /lignin sample were found to be symmetrical and to cross the origin, indicating that there is no coercivity in the magnetic lignin. This hysteresis loop did not exhibit remanence or hysteresis, indicating that the magnetic  $\text{Fe}_3\text{O}_4$ /lignin mixture that was prepared had good super-paramagnetism. In particular, the saturation magnetization values for  $\text{Fe}_3\text{O}_4$  and  $\text{Fe}_3\text{O}_4$ /nanolignin were 72.9 and 50.8  $\text{emu}\cdot\text{g}^{-1}$ ,

respectively. The findings suggested that a higher lignin loading could reduce the magnetic strength of the  $\text{Fe}_3\text{O}_4$ . The non-magnetic nature of lignin's coating provides an explanation for this phenomenon. Increased coatings will cause  $\text{Fe}_3\text{O}_4$  nanoparticles' dipole moment to rise and their magnetic content to fall, which will reduce their magnetic properties.  $\text{Fe}_3\text{O}_4$ /lignin maintains the super-paramagnetic characteristics even though its magnetic strength decreases, and it is still strong enough to be magnetically separable when a magnetic field is applied. The outcome demonstrates how the  $\text{Fe}_3\text{O}_4$ /lignin nanoparticles' super-paramagnetic property provides an ideal environment for keeping them from aggregating and enabling them to quickly re-disperse when the magnetic field is removed, both of which are essential for their use in the biomedical field.



**Figure 5. Magnetization curves of (a)  $\text{Fe}_3\text{O}_4$  and (b)  $\text{Fe}_3\text{O}_4/\text{nanolignin}$**

#### 4. CONCLUSIONS

The study has successfully synthesized  $\text{Fe}_3\text{O}_4$  nanoparticles by incorporating lignin extracted from bagasse with optimal parameters such as the ratio between  $\text{Fe}_3\text{O}_4$  nanoparticles and lignin of 1:0.5, reaction time of 9 hours. The obtained material is spherical, has an average size of  $53.42 \pm 5.12$  nm (results from SEM images) and the particle diameter distribution is relatively uniform. The thermal stability in both grades is quite stable. The magnetic

saturation of  $\text{Fe}_3\text{O}_4$  nanoparticles and  $\text{Fe}_3\text{O}_4/\text{lignin}$  materials was determined by a vibrating sample magnetometer (VSM) with values of 72.9 and 50.8  $\text{emu}\cdot\text{g}^{-1}$ , respectively, which is critical for their application in the drug delivery field.

#### ACKNOWLEDGMENTS

This study is funded in part by the Can Tho University, Code: T2022-04.

#### REFERENCES

- Arni, S. A. (2018). Extraction and isolation methods for lignin separation from sugarcane bagasse: a review, *Industrial Crops and Products*, 115, 330-339.
- Ba-Abbad, M. M., Benamour, A., Ewis, D., Mohammad, A. W., & Mahmoudi, E. (2022). Synthesis of  $\text{Fe}_3\text{O}_4$  nanoparticles with different shapes through a co-precipitation method and their application, *Journal of the Minerals*, 74, 3531–3539.
- Figueiredo, P., Lintinen, K., Kiriazis, A., Hynninen, V., Liu, Z., Bauleth-Ramos, T., Rahikkala, A., Correia, A., Kohout, T., Sarmiento, B., Yli-Kauhaluoma, J., Hirvonen, J., Ikkala, O., Kostianen, M. A., & Santos, H. A. (2017). In vitro evaluation of biodegradable lignin-based nanoparticles for drug delivery and enhanced antiproliferation effect in cancer cells. *Biomaterials*, 121, 97-108.
- Ha, B. T., Thanh & H. T. (2017). Synthesis of  $\text{Fe}_3\text{O}_4/\text{SiO}_2$  adsorbent materials used to treat Cr(VI) in wastewater, *Journal of Science Technology and Food*, 12, 43 – 49.
- Hanh, C. L. N., Thanh, L. H. V., Tuan, N. T., Thuyen, N. T. B., Mai, N. T. N., Huyen, N. T. M., & Tan, V. D. (2022). Size-controlled synthesis of lignin particles from sugarcane bagasse supported by probe-type sonication, *Can Tho University Journal of Science*, 58(2), 51-65.
- Hasany, S. F., Abdurahman, N. H., Sunarti, A. R., & Jose, R. (2013). Magnetic Iron oxide nanoparticles: chemical synthesis and applications review, *Current Nanoscience*, 9, 561-575.
- Hoa, N. T., Tuong, N. M., & Phuong, N. T. (2020). Study on fabrication of composite materials based on nano chitosan/ $\text{Fe}_3\text{O}_4$  applied to lead treatment in aqueous solution, *Journal of Military Science and Technology*, 9, 205 – 211.
- Huang, C., Pei, W., Shang, W., Liang, C., & Yong, Q. (2020). Using lignin as the precursor to synthesize  $\text{Fe}_3\text{O}_4/\text{lignin}$  composite for preparing electromagnetic wave absorbing lignin – phenol – formaldehyde adhesive, *Industrial Crops and Products*, 154(6), 1126368.
- Kim, Y. S., & Kadla, J. F. (2010). Preparation of a thermoresponsive lignin-based biomaterial through

- atom transfer radical polymerization, *Biomacromolecules*, 11(4), 981–988.
- Liu, K., Zheng, D., Lei, H., Liu, J., Lei, J., Wang, L., & Ma, X. (2018). Development of novel lignin-based targeted polymeric nanoparticle platform for efficient delivery of anticancer drugs, *ACS Biomaterials Science and Engineering*, 4(5), 1730–1737.
- Min, D., Zhang, Q., Li, M., Guo, C., Wan, G., Jia, Z., & Wang, S. (2019). Fe<sub>3</sub>O<sub>4</sub> nanoparticles loaded on lignin nanoparticles applied as a peroxidase mimic for the sensitively colorimetric detection of H<sub>2</sub>O<sub>2</sub>, *Nanomaterials*, 9(2), 210.
- Pei, W., Shang, W., Liang, C., Jiang, X., Huang, C., & Yong, Q. (2020). Using lignin as the precursor to synthesize Fe<sub>3</sub>O<sub>4</sub>@lignin composite for preparing electromagnetic wave absorbing lignin-phenol-formaldehyde adhesive, *Industrial Crops and Products*, 154, 112638.
- Thanh, L. H. V., Han, K. G., Han, N. N., Pha, B. Y., & Mai, N. T. N. (2021). Synthesis of Fe<sub>3</sub>O<sub>4</sub>@SiO<sub>2</sub> attached Fe<sup>0</sup> and its treatment of methyl blue in aqueous solution, *Can Tho University Journal of Science*, 57(4), 40-52.
- Thang, N. Q., Quang, H. D., Le, T. C., & Hien, L. T. T. (2019). Characterization of structure, morphology, properties, Fe<sub>3</sub>O<sub>4</sub> magnetic nanoparticles synthesized by thermal decomposition method, *Vinh University Journal of Science*, 47, 55 – 62.
- Vasquez, E. S., Petrie, F. A., Gorham, J. M., Busch, R. T., & Leontsev, S. O. (2021). Facile fabrication and characterization of kraft lignin@Fe<sub>3</sub>O<sub>4</sub> nanocomposites using pH driven precipitation: Effects on increasing lignin content, *International Journal of Biological Macromolecules*, 181, 313 – 321.
- Zhao, J., Zheng, D., Tao, Y., Li, Y., Wang, L., Liu, J., He, J., & Lei, J. (2020). Self-assembled pH-responsive polymeric nanoparticles based on lignin-histidine conjugate with small particle size for efficient delivery of anti-tumor drugs, *Biochemical Engineering Journal*, 156, 107526.